ICEMG 2023-XXXXX

Improving the Current Controller Performance Based on Model Predictive Control in the Mono-Inverter Dual-Parallel System

Mehdi fadaie[1], **Karim abbaszadeh**[2,†], **Alireza siadatan**[3]

[1]Department of Electrical Engineering, Faculty of Electrical Engineering, Science and Research Branch, Islamic Azad University, Tehran, Iran.
[2]Department of Electrical Engineering, Faculty of Electrical Engineering K. N. Toosi University of Technology, Tehran, Iran.
[3]Department of Electrical Engineering, College of Technical and Engineering West Tehran Branch, Islamic Azad University, Tehran, Iran

Abstract
Using the structure of the dual-parallel motors fed by mono-inverter is developing in electric trains and cars for reasons such as managing energy consumption and reducing the volume, weight, and cost of electric motor drives. The major problem in this structure, also called Mono-Inverter Dual Parallel (MIDP), is the design of the current controller in the unequal load torque conditions of the motors because of the same voltage applied to dual-parallel motors. Therefore, the Predictive Current Controls (PCC) have been proposed in two classes, Finite Control Set Model Predictive Control (FCS-MPC) and Continuous Control Set MPC (CCS-MPC). This paper compares the performance of the current controller designed based on FCS-MPC with the controller designed based on the latest method introduced in the CCS-MPC category. The simulation results confirm the novel method performance from the point of view of the amount of disturbance produced in the current and load torque waveforms.

Keywords: predictive current controller, finite control set model predictive control, continuous control set model predictive control, mono-inverter dual- parallel, permanent magnet synchronous motor.

Introduction
Multi-Machine systems have become prevalent in some devices to provide mechanical propulsion as electric vehicles and urban trains. An efficient method for managing energy consumption and optimizing the dimensions and costs of the multi-machine system is feeding parallel motors with one three-leg inverter, called Mono-Inverter Dual-Parallel (MIDP) system. The inverter's shared legs between two electric motors are switched to either the pulse-wide modulation (PWM) or the space vector modulation (SVM) method. Since permanent magnet synchronous motors (PMSM) have high power density, high torque per ampere ratio, and high efficiency, they are used in MIDP systems commonly [1]. Parallel motors are driven by the cascade method, in which a proportional-integral (PI) controller is typically used in the outer loop to control the speed of the electric motors, and a current controller is used in the inner loop. Figure 1 shows the diagram block of the MIDP system drive. One of the issues discussed in the MIDP system is the current controller design so that both motors can properly operate under unequal load torque conditions.

In this regard, two methods of weighted average and Master-Slave (MS) were introduced to produce internal loop control signals [2, 3]. However, eliminating fluctuations and maintaining the stable performance of motors are the principal concerns. The reduced-order feedback linearization was another design approach for the current controller that could hardly control the system at singular points [4]. The Direct Torque Control (DTC) method was introduced in the MIDP system [5]. However, the ambiguous process of determining the suitable voltage vectors from the switching lookup table is one of its drawbacks. With the development of microcontroller manufacturing technology, the Predictive Current Controller (PCC) method was used in driving electric motors [6]. Typically, there are two general approaches to executing the PCC methods for the MIDP system. The first approach, called Finite Control Set Model Predictive Control (FCS-MPC), was applied on two PMSM motors and two induction motors in [7, 8] and [9-11], respectively. This method uses just six well-known voltage vectors in SVM to minimize the cost function. These vectors have the same amplitude with an angle difference of 60 degrees relative to each other [12]. Certainly, the lowest value of the cost function is not obtained by six voltage vectors, and it is necessary to consider all of the voltage space vectors [13]. The second approach is the Continues Control Set-Model Predictive Control (CCS-MPC) method [14]. The CCS-MPC method, using one of the optimal control methods, solves the cost function by considering some limitations and the system's initial conditions. Pontryagin's maximization principle has been recently used in the current controller design [15]. Solving the optimization problem by this method has led to obtaining an explicit function for voltage control signals according to control variables and system states. Also, the computational volume has been reduced, and control signals have resulted in optimal system behavior. However, this reference has evaluated the designed current controller together with the speed controller, which has a different structure from conventional PI controllers. Therefore, this paper, considering the speed controller of the conventional PI in the outer loop, compares the current controller performance designed based on Pontryagin's maximum principle with the one based on the finite control set (FCS) method. This paper is organized as follows. In the first part, the MIDP system structure is explained. In the second part, a summary of designing the current controller process is explained in the FCS-MPC and CCS-MPC

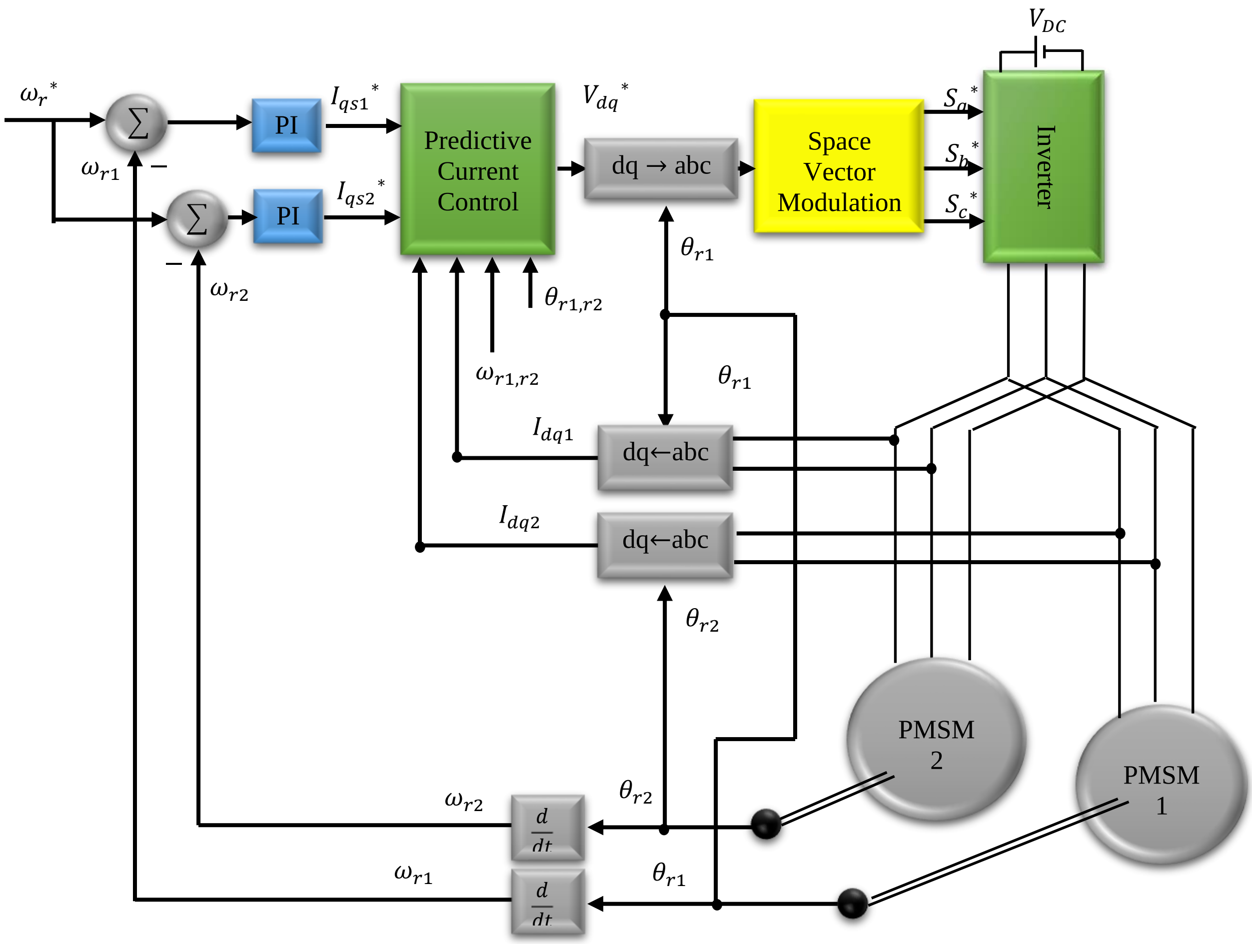

Figure 1. The block diagram of the mono-inverter dual-parallel PMSM motors.

methods. Then, how to produce the voltage signals in two methods is compared. In the next section, the simulation results of the two methods are presented and compared in the Simulink MATLAB environment. Finally, a conclusion is presented.

The Structure of MIDP System

Figure 1 is shown the closed-loop control of two PMSM motors with common feeding from a three-phase inverter. Two conventional PI controllers in the outer loop are obliged to adjust the speed of the motors and track the reference speed. Also, the current controller in the inner loop is responsible for tracking the control signals of the outer loop. Then, the voltage control signals produced by the inner circle generate the switching pulses which are applied to the inverter using the SVM method. Both PMSM motors have the identical specifications. In order to design a proper and unit current controller, both of them should be presented in a synchronous frame. According to the reference model of motors in [13, 15], the discrete-state model of them in the rotor reference frame of the first motor will be as follows:

$$\begin{cases}\begin{bmatrix} I^{r_1}_{qds1}(k+1)\\ I^{r_1}_{qds2}(k+1)\end{bmatrix} = \begin{bmatrix}\gamma_1 & 0\\ 0 & \gamma_2\end{bmatrix}\begin{bmatrix} I^{r_1}_{qds1}(k)\\ I^{r_1}_{qds2}(k)\end{bmatrix} + \cdots \\ \qquad \ldots + \gamma_3 \begin{bmatrix}1\\1\end{bmatrix} V^{r_1}_{qds}(k) + \begin{bmatrix}0\\ \gamma_4\end{bmatrix}; \end{cases} \tag{1}$$

where $\gamma_1, \gamma_2, \gamma_3$ and γ_4 are presented in appendix.

Finally, the closed-loop control is completed by sensing the rotor position of the motors.

Summary of designing the PCC controllers

There are two known approaches in the design of the current controller using the predictive method, and the difference between them is how to minimize the cost function. The FCS-MPC method could find the minimum value of the cost function by considering a limited number of control signals. However, the CCS-MPC method, by solving the optimization problem, could obtain an expression for the control signal, which causes the cost function to be minimized. The general principles of each method are explained in the following.

Finite Control Set Model Predictive Control (FCS-MPC)

FCS-MPC is a well-known method used in the design of the current controller in both single-motor and multi-motor systems due to the simplicity in design, no need for a modulator, and low calculation time for generating control signals. The cost function is usually considered a quadratic function of the state variables in multi-motor systems as follows:

$$CF = Min \sum_{j=1}^{2}\left[K_{\psi_j}\left|\hat{I}_{ds_j} - I^{r_1}_{ds_j}\right|^2 + K_{T_j}\left|\hat{I}_{qs_j} - I^{r_1}_{qs_j}\right|^2\right]; \tag{2}$$

where $\hat{I}_{\mathrm{ds}}$ is the reference value of the flux-component current of each motor, and $\hat{I}_{\mathrm{qs}}$ is the control signal of each speed controller, or in the other words, is the torque-component current of each motor. The state variables of the $I_{\text{ds}}^{r_1}$ and $I_{\text{qs}}^{r_1}$ are obtained by Eq. (1) for each vector voltages. As shown in Figure 2, there are six vector voltages. Therefore, six current vectors, $I_{\text{qds}}^{r_1}(k+1)$, are produced duo to voltage vectors. As a result, a voltage vector is obtained that minimizes the cost function after 24 times calculating the electrical equations of motors and six times calculating the cost function at each sampling time. As it can be concluded, a definite function cannot be given for voltage control signals.

Continuous Control Set Model Predictive Control (CCS-MPC)

Designing controllers based-MPC has wide varieties. Among them, the CCS-MPC method is more interesting because it can provide an explicit control law for the controlled system. A quadratic cost function is often considered in this method, as follows:

$$\mathcal{J} = Min\frac{1}{2}\left[\left(X(t_f)-\hat{X}\right)^T Q_f\left(X(t_f)-\hat{X}\right)+\int_{t_i}^{t_f}\left(X(t)-\hat{X}\right)^T Q(X(t)-X^*)+U^T(t)RU(t)d\tau\right]; \tag{3}$$

where $Q \geq 0$, $Q_f \geq 0$ and $R > 0$ are weighting matrices to be selected, $\hat{X}$ is the reference state vector, X is the optimal value of the state vector, t_f is the end of the predictive horizon, and $X(t_f)$ is the state vector at t_f. The first statement is the final cost function and the other is the integral cost function. By having the controlled system model and its constraints, solving the predictive control problem can be considered equivalent to solving the optimal control problem for the current controller design. Reference [15] has used Pontryagin's Maximum Principle to design the current controller by the CCS-MPC method. By writing Pontryagin's function in terms of control variables and reference values and considering the necessary optimization conditions, this article obtains the differential equations for the current controller design. These equations are as follows:

$$\begin{cases} X^\bullet(t) = A\left(X(t_i)\right)X(t) - BU(t) + D(X(t_i), t_i); \\ \psi^\bullet(t) = -Q\left(X(t)-\hat{X}\right) - A^T\left(X(t_i)\right)\psi(t); \\ U(t) = R^{-1}B^T\psi(t); \\ X(t_i) = X_{t_i}; \\ \psi(t_f) = \left(\frac{\partial\left(X(t_f)-\hat{X}\right)^T Q_f\left(X(t_f)-\hat{X}\right)}{\partial X(t)}\right) = Q_f\left(X(t_f)-\hat{X}\right); \end{cases} \tag{4}$$

The obtained equations were presented in terms of state variables and quasi-variables. Since the general solution of the differential equation requires two sets of certain conditions, the values of the state variables at the beginning of the optimization window and the pseudo-state variables at the end of the prediction horizon had been selected as boundary conditions. By using the forward Euler approximation and after simplifications, the voltage control signals were presented as an explicit function of the state variables. These signals are as follows:

$$\begin{bmatrix} V_{qs}^{r_1} \\ V_{ds}^{r_1} \end{bmatrix} = \alpha \begin{bmatrix} I_{qds_1}^{r_1} \\ I_{qds_2}^{r_1} \end{bmatrix} + \beta^{(1)} \begin{bmatrix} \hat{I}_{qds_1}^{r_1} \\ \hat{I}_{qds_2}^{r_1} \end{bmatrix} - \beta^{(2)}\left(\frac{\psi_f}{L}\right)\left[\omega_{r_1} \quad 0 \quad \omega_{r_2}\cos(\theta_r') \quad \omega_{r_2}\sin(\theta_r')\right]^T; \tag{5}$$

where α , $\beta^{(1)}$ and $\beta^{(2)}$ are 2×4 matrices in term of ω_{r_1}. Also, ψ_f and L are the linkage flux and synchronous inductance, respectively. As can be seen in Eq. (5), the control signals are obtained as linear-parametric relations from the measurable state variables.

Comparison of the produced voltage control signal in FCS-MPC and CCS-MPC methods

The main issue in the design of the current controller for the MIDP system is that only one voltage vector is available to control both motors. If the load torque in the motors is equal, both motors have the same behavior. As a result, motors will be considered as one motor from the point of view of the current controller. Therefore, one voltage vector can control both motors. However, the control of motors with a voltage vector will be complicated in unbalanced torque. In order to explain the problem, it is assumed that the first motor with $\vec{V}_{qds1}$ voltage vector and the second motor with $\vec{V}_{qds2}$ will be able to control both motors under unbalanced torque conditions properly. These vectors are displayed in the space voltage vector in Figure 2.

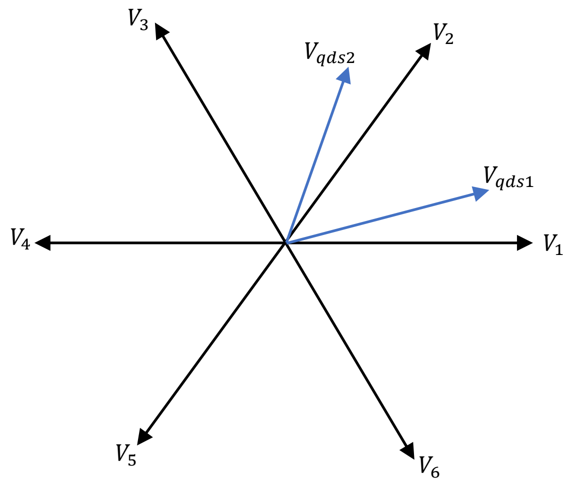

Figure 2. Control signals in space voltage vector

Notice that the angle difference between the voltage vectors is a function of the load torque difference in motors. The main challenge in predictive current controllers, regardless of their design method, is to produce the control signal in the space voltage vector so that this signal is as close as possible to the $\vec{V}_{qds1}$ and $\vec{V}_{qds2}$ vectors and minimizes the predefined cost function. The current control, designed in the FCS method, has only six voltage control signals ($V_1, V_2, \ldots, V_6$) shown in Figure 2. Due to the limited number of control signals in FCS-MPC, its voltage control signals cannot coincide with $\vec{V}_{qds1}$ and $\vec{V}_{qds2}$ vectors, and they can match in the best case over the voltage vector of one of the motors. The amplitude of six voltage vectors is also constant, which leads to the maximum use of the inverter's ability in situations where such a voltage amplitude is not needed. Although the FCS-MPC method does not require a modulator and does not require complex calculations to produce a control signal, tracking the generated command signals in the outer loop will not be realized appropriately.

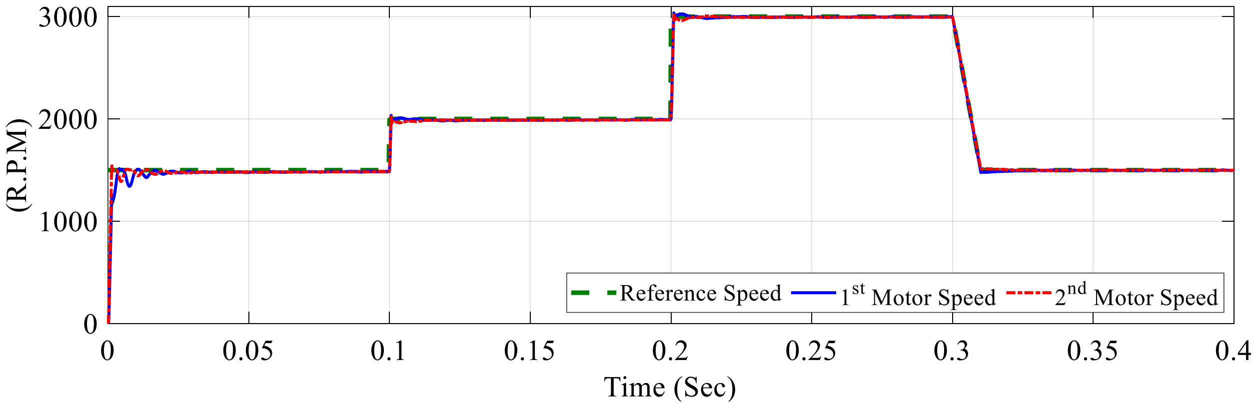

(a)

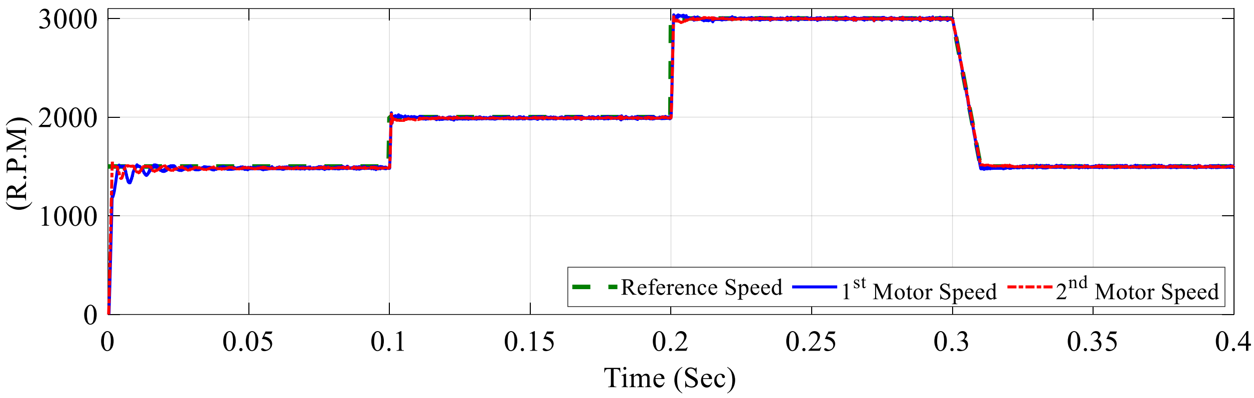

(b)

Figure 3. A general view of the speed change of motors in unbalanced torques. (a) CCS-MPC method. (b) FCS-MPC method.

This matter can appear as a disturbance in the current and torque waveforms.

Unlike the FCS-MPC method, the current controller designed by the CCS-MPC evaluates the entire space voltage vector to generate the appropriate voltage vector. This feature ensures the proper performance of the motors and minimizes the cost function. In addition, this controller will not use the maximum capability of the inverter in any situation. Therefore, it has lower switching losses compared to the controller designed in the FCS-MPC method. Other advantages of this current controller include accurate tracking of the command signals generated in the outer loop and less distortion of torque and current waveforms. However, the main problem in this type of controller is a large number of calculations that spend lots of computational time to obtain a suitable control signal. Fortunately, this problem has been solved with efficient techniques such as Pontryagin's Maximum Principle.

Results and Discussion

To show the performance and capability of the proposed controller, MATLAB / Simulink software is used to run the proposed drive technique. Two identical PMSM motors manufactured by LS Company with XML-SB04A series are chosen as MIDP system motors. The specifications are listed in Table 1. The specifications of the SVM modulation inverter are listed in Table 2. The weighting matrices in CCS-MPC are selected as follows:

$$R = \begin{bmatrix} 1 & 0 \\ 0 & 1 \end{bmatrix}; \quad Q = \begin{bmatrix} 15 & 0 & 0 & 0 \\ 0 & 85 & 0 & 0 \\ 0 & 0 & 15 & 0 \\ 0 & 0 & 0 & 85 \end{bmatrix};$$

Table 1. PMSM motor parameters

Motor Parameter		Parameter Value
Nominal Power	P_{rate}	400^{Watt}
Nominal Current	I_{rate}	2.89^{A}
Pole Number	p	8
Stator Resistance	r_s	0.82^{Ω}
Stator Inductance	L	3.66^{mH}
Permanent Magnet Flux	ψ_f	0.0734^{wb}
Nominal Speed	N_{syn}	$3000^{r.p.m}$
Nominal Torque	T_{rate}	$1.27^{\,N.m}$
Maximum Torque	T_{max}	$3.82^{\,N.m}$
Moment of Inertia	J	$0.0321 \times 10^{-4}\ {}^{Kg.m^2}$
Friction Coefficient	B_m	$0.6 \times 10^{-6}\ {}^{N.m.Sec}$

Table 2. Three-phase inverter parameters

Inverter Parameter		Parameter Value
DC Power Supply	V_{DC}	173^{V}
Switching Frequency	f_{SW}	8^{KHz}
On-Mode Resistance	$R_{DS(on)}$	0.019^{Ω}

$$Q_f = \begin{bmatrix} 280 & 0 & 0 & 0 \\ 0 & 5800 & 0 & 0 \\ 0 & 0 & 280 & 0 \\ 0 & 0 & 0 & 5800 \end{bmatrix};$$

The K_ψ and K_T have been selected as 0.01 and 0.11, respectively. Both control methods have the same speed control loop, as their PI coefficients are $K_P = 0.766$ and $K_I = 4$, respectively. The speed waveforms of both methods are shown in Figure 3. The process of changing the speed of the motors has been done in unbalanced load torque, so that the load torque of the first motor is at the

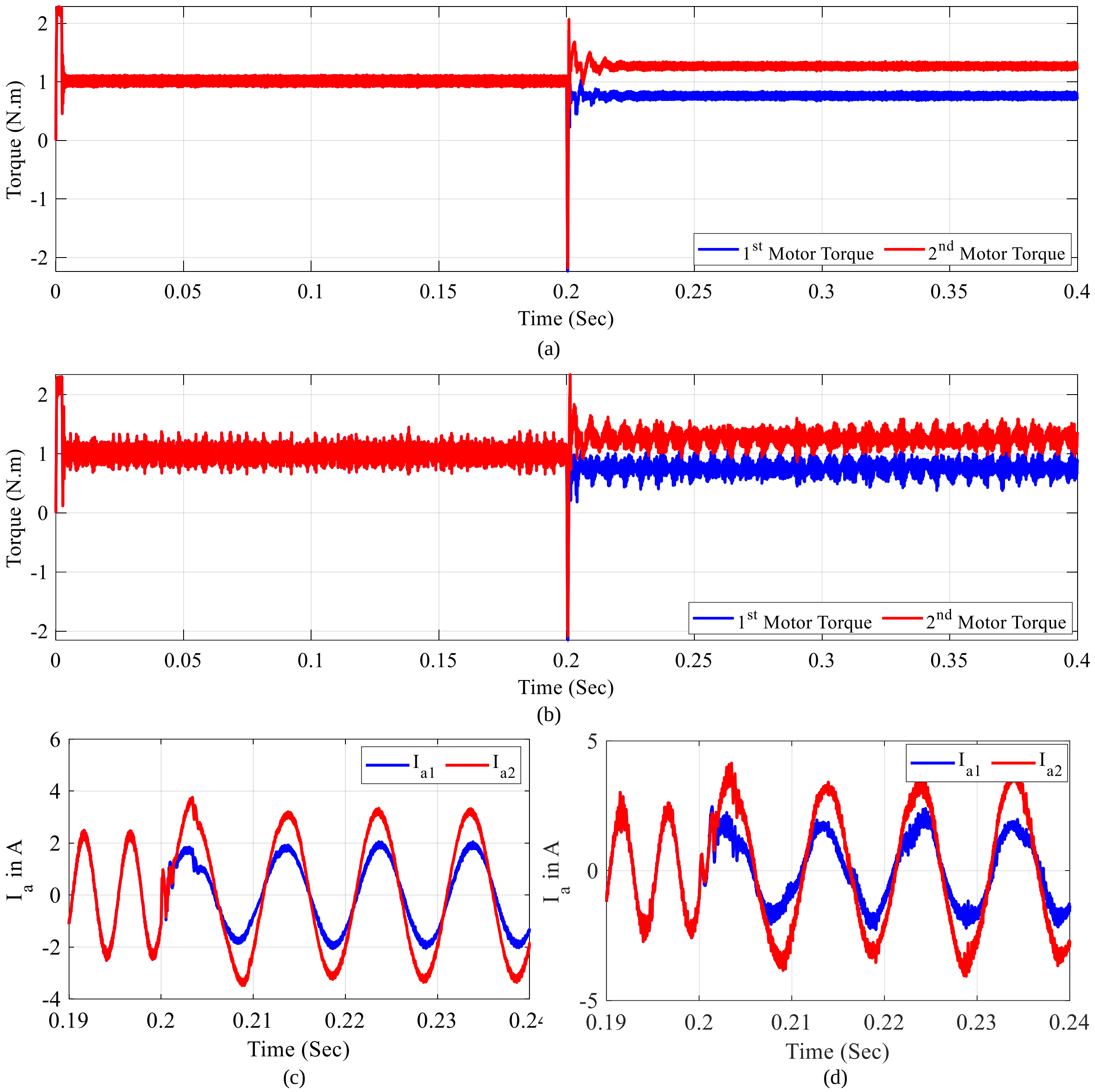

Figure 4. The torque and current waveforms in both methods. (a) The torque waveform of motors in CCS-MPC. (b) The torque waveform of motors in FCS-MPC. (c) and (d) The phase-a current waveform of motors in CCS-MPC and FCS-MPC, respectively.

nominal value and the second motor is at 80% of its value. The speed response of both methods is similar because the type of speed controllers is the same in the outer loop.

The performance difference of the current controllers could be investigated in the torque and current responses. Figure 4 shows the torque and current waveform. Motors are started with rated speed and 80% of rated torque. The speed of motors is halved in 0.2 seconds, and their torque changes by 20%. Indeed, the first motor load torque is reduced to 60% of the rated value, and the second motor is increased to the rated torque. As shown in Figure 4, the amount of ripple in torque and current waveforms in the current controller designed by the FCS method is much higher than its value in the current controller designed by the CCS method. Table 3 presents the numerical comparison of the amount of distortion in two methods. The amount of distortion has been compared by calculating the integral square error (ISE) in the torque waveform and the THD in the current waveform.

Table 3. The THD and MSE comparison of the torque and current in two methods.

	Balance Conditions		Unbalance Conditions	
	CCS	FCS	CCS	FCS
	ISE		ISE	
T_1	0.0020	0.01140	0.000847	0.00750
T_2	0.0020	0.01140	0.000847	0.00740
	THD		THD	
I_{a1}	%4.810	%10.920	%3.900	%15.50
I_{a2}	%4.810	%10.920	%2.310	%6.97

The MSE is calculated as follows:

$$ISE_k = \sum \left(T_{e,k} - T_{L,k}\right)^2 \Delta t \,; \qquad k = 1,2 \tag{6}$$

where $T_{e,k}$ is the kth motor torque and $T_{L,k}$ is the kth load torque. It can be seen that the CCS-based current controller performance both in balanced and unbalanced conditions is more acceptable than the FCS. Therefore, the CCS-based current controller is preferred in the MIDP system. Notice that elapsed time to generate the control signal in this method is an important issue. As calculated in [15], the elapsed time is 0.007535^{ms} in the introduced CCS method, while it is about 0.013147^{ms} for the FCS method. As a result, the CCS-MPC method is approximately 1.745 times less time-consuming than the FCS-MPC method.

Conclusions

This paper focuses on designing the current controller based on MPC in the inner loop of the MIDP system drive. The results confirm that the FCS method cannot have suitable dynamics for the MIDP system with six voltage vectors with constant amplitude and angle. The distortion in the waveforms and the larger amplitude of the currents indicate this problem. But the simplicity of this method and the short computing time in producing the voltage signal are the factors that interest research on FCS-based controllers. On the other hand, it was observed that the CCS-based current controller has a relatively more calculation process. However, the computing time in producing the voltage control signal, distortion in the waveforms, and the amplitude of the currents have been reduced significantly. As a result, using the introduced CCS method can be more efficient than the FCS method in the MIDP system.

Appendix

$$\gamma_1 = \gamma_2 = \begin{bmatrix} -\frac{r_s}{L} & -\omega_{r1} \\ \omega_{r1} & -\frac{r_s}{L} \end{bmatrix}; \quad \gamma_3 = \frac{1}{L}\begin{bmatrix} 1 & 0 \\ 0 & 1 \end{bmatrix};$$

$$\gamma_4 = -\frac{\psi_f}{L}\omega_{r2}\begin{bmatrix} cos(\theta_r') \\ sin(\theta_r') \end{bmatrix};$$

References

[1] W. Cai, X. Wu, M. Zhou, Y. Liang, and Y. Wang,(2021), "Review and development of electric motor systems and electric powertrains for new energy vehicles," *Automotive Innovation,* vol. 4, no. 1, pp. 3-22, Art no.

[2] J. M. Lazi,(2020), "Non-independent speed control for dual-PMSM drives fed by a single three-leg VSI," vol. 20, pp. 1717-1724, Art no.

[3] T. Ahmed, H. Kada, and A. Allali,(2020), "New DTC strategy of multi-machines single-inverter systems for electric vehicle traction applications," *International Journal of Power Electronics and Drive Systems,* vol. 11, no. 2, p. 641, Art no.

[4] T. Liu, X. Ma, F. Zhu, and M. Fadel,(2021), "Reduced-order feedback linearization for independent torque control of a dual parallel-PMSM system," *IEEE Access,* vol. 9, pp. 27405-27415, Art no.

[5] M. Fadel, N. L. Nguyen, and A. Llor, "Direct Torque Control—A solution for mono inverter-dual parallel PMSM system," in *21st Mediterranean Conference on Control and Automation*, 2013: IEEE, pp. 1477-1483.

[6] J. Rodriguez *et al.*,(2021), "Latest advances of model predictive control in electrical drives—Part II: Applications and benchmarking with classical control methods," *IEEE Transactions on Power Electronics,* vol. 37, no. 5, pp. 5047-5061, Art no.

[7] Z. Yu, Z. Du, W. Wang, and X. Gu, "Model Predictive Control Method of Dual PMSM Fed by Single Inverter Based on MTPA," in *2020 Chinese Automation Congress (CAC)*, 2020: IEEE, pp. 1477-1482.

[8] C. Park and S. Doki,(2022), "Active Damping Control Method for Different Dual-Parallel-SPMSM Systems with Single Inverter," *IEEJ Journal of Industry Applications,* p. 22006418, Art no.

[9] A. A. Adam, A. Purwadi, and A. S. Rohman, "Dual Parallel Induction Motor Fed by a Single Inverter Based On Two Step Predictive Torque Control."

[10] Š. Janouš, J. Talla, Z. Peroutka, and V. Šmídl, "Predictive control of parallel induction motors fed by single inverter with common current sensors," in *IECON 2018-44th Annual Conference of the IEEE Industrial Electronics Society*, 2018: IEEE, pp. 5843-5848.

[11] M. A. Abbasi and A. R. B. HUSAIN,(2018), "Model predictive control of a dual induction motor drive fed by a single voltage source inverter," *Turkish Journal of Electrical Engineering and Computer Sciences,* vol. 26, no. 3, pp. 1623-1637, Art no.

[12] M. K. Ratib *et al.*,(2022), "Applications of hybrid model predictive control with computational burden reduction for electric drives fed by 3-phase inverter," *Ain Shams Engineering Journal,* p. 102028, Art no.

[13] M. Fadaie Abras, K. Abbaszadeh, and A. Siadatan, "An Energy-based Predictive Control with a Fast Real-Time Current-Tuning for Mono-Inverter Dual-Parallel PMSM Motors in Power Train Application," *Journal of Control (English Edition),* pp. 0-0, Art no.

[14] A. Cervone, L. Di Noia, R. Rizzo, I. Spina, and R. Miceli, "A Constrained Optimal Model Predictive Control for Mono Inverter Dual Parallel PMSM Drives," in *2018 7th International Conference on Renewable Energy Research and Applications (ICRERA)*, 2018: IEEE, pp. 1501-1507.

[15] M. Fadaie, K. Abbaszadeh, and A. Siadatan,(2022), "Simplified and Accurate Predictive Control Method in Mono-Inverter Dual-Parallel Permanent Magnet Synchronous Motors," *International Journal of Industrial Electronics Control and Optimization,* vol. 5, no. 3, pp. 251-260, Art no.